

Maroua Jaoua

Bachelor Thesis 2017 supervised by:
Dr. Siroos Azizmohammadi

Solution to Buckley-Leverett Problem

*I dedicate this thesis to my family, my professors and my friends
who have supported me through the process*

Declaration

I hereby declare that except where specific reference is made to the work of others, the contents of this dissertation are original and have not been published elsewhere. This dissertation is the outcome of my own work using only cited literature.

Erklärung

Hiermit erkläre ich, dass der Inhalt dieser Dissertation, sofern nicht ausdrücklich auf die Arbeit Dritter Bezug genommen wird, ursprünglich ist und nicht an anderer Stelle veröffentlicht wurde. Diese Dissertation ist das Ergebnis meiner eigenen Arbeit mit nur zitierter Literatur.

Maroua Jaoua, 13 March 2017

Acknowledgements

I would like to express my deep appreciation and indebtedness to my advisor Dr. Siroos Azizmohammadi for his particular assistance and guidance and I would also like to thank Mr. Zar Hichem for his support and help.

I also wish to express my sincere gratitude to my parents and friends for their endless encouragement and care.

Abstract

Waterflooding is one of the most reliable recovery methods that are utilized to increase the oil production rates and oil recovery. In a one-dimensional, incompressible and multiphase petroleum reservoir, it is well described by Buckley Leverett theory. Therefore, in this thesis, the Buckley Leverett equation is initially derived and solved with neglecting the effects of gravity and capillary pressure. The results from the analytical and the numerical solutions are also compared and possible ways to improve the numerical method were suggested. Then, to understand the effects of capillarity and gravity, Buckley Leverett equation was extended and the parameters that influence the saturation profile and the fractional flow curve were discussed. For both cases, the mathematical and physical aspects were explained.

Key words: Waterflooding, Multiphase flow, Buckley Leverett equation, Generalized Buckley Leverett equation, Analytical solution, Numerical solution

Zusammenfassung

Wasserflutung ist einer der verlässlichsten Recovery-Methoden, die angewendet werden um die Ölproduktionsraten sowie die Ölgewinnung zu erhöhen. In einem eindimensionalen, inkompressiblen und mehrphasigen Petroleumreservoir wird diese Methode durch die Buckley Leverett Theorie sehr gut beschrieben.

Daher wird in dieser Arbeit zunächst die Buckley-Leverett-Gleichung abgeleitet und gelöst wobei die Effekte von Schwerkraft und Kapillardruck vernachlässigt werden. Die Ergebnisse der analytischen und numerischen Lösungen werden ebenfalls verglichen und ebenso Wege zur Verbesserung der numerischen Methode suggeriert. Um die Auswirkungen der Kapillarität und Schwerkraft zu verstehen, wurde die Buckley Leverett-Gleichung erweitert. Die Parameter, die das Sättigungsprofil und die Bruchkurve beeinflussen, wurden anschließend analysiert. Für beide Fälle werden die mathematischen und physikalischen Aspekte behandelt.

Key words: Wasserflutung, Mehrphasenströmung, Buckley Leverett Gleichung, Generalisierte Buckley Leverett Gleichung, Analytische Lösung, Numerische Lösung.

Table of Contents

Declaration.....	iii
Erklärung	iii
Acknowledgements.....	iv
Abstract.....	v
Zusammenfassung.....	vi
Chapter 1	1
Introduction.....	1
1.1 Background and Context.....	1
1.2 Scope and Objectives.....	1
Chapter 2.....	3
Literature Review.....	3
Chapter 3.....	5
The Basic Theory of Buckley-Leverett.....	5
3.1 Fractional flow equation	5
3.2 Frontal advance equation	8
3.3 Buckley-Leverett Solution.....	10
Chapter 4.....	23
Generalized Buckley-Leverett Equation.....	23
4.1 Gravity Effect.....	23
4.2 Capillary Pressure Effect	25
Chapter 5.....	31
Conclusion	31
5.1 Summary	31
5.2 Future Work.....	32
Chapter 6.....	33
References.....	33

List of Figures

Figure 1: Linear displacement in an inclined system.....	6
Figure 2: Water flow through a linear differential element	9
Figure 3: Velocity corresponding to a constant saturation ($dS=0$ or $S=S_b$) at (x,t) plane	11
Figure 4: Corey Relative Permeability	12
Figure 5: Fractional Flow curve.....	12
Figure 6: Derivative of Fractional Flow	14
Figure 8: Saturation Profile, Unphysical Solution	14
Figure 9: Saturation Profile at different times	15
Figure 10: Spreading Wave	16
Figure 11: Indifferent wave	16
Figure 12: Self-sharpening wave resulting in a shock wave.....	16
Figure 13: The Buckley-Leverett wave	16
Figure 14: Saturation Profile, Physical Solution.....	17
Figure 15: Illustration of the average water saturation	18
Figure 16: Graphical Determination of Front Saturation.....	19
Figure 17: Saturation Profile, Physical solution	19
Figure 18: Dimensional core space discretization	20
Figure 19: Saturation Profile, Numerical Solution	21
Figure 20: Comparison between the analytical and numerical solutions.....	22
Figure 21: Effect of changing gravity number on the fractional flow curve	24
Figure 22: Space and time discretization	28
Figure 23: Saturation Profile with Capillary Pressure Effect.....	29
Figure 24: Saturation Profile without Capillary Pressure	29

List of Tables

Table 1: Pore types in soils	A-3
------------------------------------	-----

Nomenclature

m	Mass	[kg]
q_o	Flow rate of oil	[m ³ /s]
q_w	Flow rate of water	[m ³ /s]
K	Absolute permeability	[m ²]
K_{ro}	Relative permeability of oil	[m ²]
K_{rw}	Relative permeability of water	[m ²]
μ_o	Viscosity of oil	[Pa·s]
μ_w	Viscosity of water	[Pa·s]
$\frac{\partial P_o}{\partial x}$	Pressure drop of oil over a given distance	[Pa/m]
$\frac{\partial P_w}{\partial x}$	Pressure drop of water over a given distance	[Pa/m]
ρ_o	Density of oil	[kg/m ³]
ρ_w	Density of water	[kg/m ³]
G	Gravitational constant	[m/s ²]
λ_o	Mobility of oil	[m ² / Pa·s]
λ_w	Mobility of water	[m ² / Pa·s]
λ_t	Total Mobility	[m ² / Pa·s]
θ	Dip angle	[°]
A	Area	[m ²]
L	Length	[m]
q_t	Total flow rate	[m ³ /s]
P_c	Capillary pressure	[Pa]
P_w	Water pressure	[Pa]
P_o	Oil pressure	[Pa]
f_w	Water fractional flow	[-]

N_G	Gravity number	
M	Mobility ratio	[-]
Φ	Porosity	[-]
Δx	Length difference	[m]
Δt	Time difference	[S]
u_w	Water velocity	[m/s]
S_w	Water saturation	[-]
S_o	Oil saturation	[-]
x_D	Dimensionless position	[-]
t_D	Dimensionless time	[-]
$\frac{\partial f}{\partial S}$	Dimensionless position in function of the water saturation	[-]
$K_{rw@Sor}$	Relative permeability of water at the residual oil saturation	[-]
$K_{ro@Swc}$	Relative permeability of oil at the connate water saturation	[-]
n_w	Corey water exponent	[-]
n_o	Corey oil exponent	[-]
S_{wi}	Initial water saturation	[-]
S_{or}	Residual oil saturation	[-]
t	Elapsed time	[s]
\bar{S}_w	Average saturation	[-]
P_w	Pressure of the wetting phase	[Pa]
P_{nw}	Pressure of the non-wetting phase	[Pa]

Chapter 1

Introduction

1.1 Background and Context

In the first stage of hydrocarbons production, the well produces naturally. Initially, the natural reservoir pressure is maintained by the primary drive mechanisms such as water drive, gas cap drive, rock and fluid expansion, solution gas drive and gravity drainage drive. The significant difference between the reservoir pressure and the bottomhole pressure drives the hydrocarbons up to the surface allowing oil recovery generally less than 30% (Abubaker H. Alagorni 2015). Nevertheless, as the reservoir pressure declines, it is necessary to supply the reservoir with external energy in order to maintain the pressure and therefore to keep the high production rates. This is referred to as secondary recovery. The most common technique of secondary recovery is waterflooding. Water is injected into the production zone through injection wells to sweep oil from the reservoir. This allows additional 30% to 50% of the oil in the reservoir to be extracted (Abubaker H. Alagorni 2015). However, in order to achieve good recovery, it is important to predict the waterflooding performance. Buckley and Leverett have investigated the special case of one dimensional, incompressible, two-phase flow system. They developed an analytical technique to calculate saturation profiles when the effects of capillary pressure and gravity are neglected.

1.2 Scope and Objectives

This thesis consists of two main parts. In the first section, the Buckley-Leverett equation is derived without accounting for the gravity and capillary pressure. An analytical solution and a numerical solution are also presented and compared. In the second section, the effects of gravity and capillary pressure are investigated leading to an expanded model.

Chapter 2

Literature Review

Waterflooding development has been increasing since the 1930s. That is because water is relatively inexpensive; usually available in adequate quantities and a reliable recovery mechanism. Therefore, the interest in the theoretical aspect of waterflooding was developed. Buckley and Leverett provided a theory for waterflooding, which investigated the case of linear, incompressible, immiscible, two-phase flow system (Buckley and Leverett 1942).

Then, Buckley and Leverett model was considered as unrealistic since it is possible to have multiple values of saturation at the same position. This limitation was overcome when Buckley and Leverett introduced the theory of shock front.

Since this improvement, multiple numerical methods were implemented to solve the Buckley-Leverett problem and to generalize it by including the effects of capillary pressure and gravity. Fayers for example examined gravity and capillarity for incompressible, two phase flow using a finite difference approximation (Fayers 1959). Gottfried was the first to present numerical solutions of three-phase flow in one-dimensional system neglecting gravity and capillary pressure (Gottfried 1966).

To link Buckley-Leverett model with the real reservoir parameters and scenarios, multiple cases were studied by different researchers. For instance, a model for non-communicating layers was developed by (Dykstra 1950), a model for communicating layers was studied by (Hiatt 1958), stratified systems with a log normal permeability distribution were also investigated based on Hiatt's theory by (Warren 1964) can be mentioned.

Chapter 3

The Basic Theory of Buckley-Leverett

The theoretical basis of Buckley Leverett model is continuum fluid mechanics, through Darcy's law and the differential form of mass balances. Therefore, the usage of such a physical machinery should be justified by determining the Knudsen number for a phenomenon involving fluid flow. In Appendix A, a back-of-the-envelope (BOTE) estimation of Knudsen number for waterflooding is provided and thus a rational behind the physical reasoning used in the main body of this thesis is provided.

Once the choice of continuum fluid mechanics is verified, the fractional flow and frontal advance equations will be derived, discussed, and solved, analytically and numerically, to predict waterflooding.

3.1 Fractional flow equation

The fractional flow equation is a model used to determine the water fraction of the total fluid flow at a particular location and time. It is also referred to as water cut. (Ahmed 2001)

The fractional flow equation is the basis of Buckley-Leverett theory. A general form of it will be demonstrated and then simplified for the purpose of this chapter. It is derived by considering the displacement of oil by water in a system of dip angle θ , area A and length L as shown in Figure 1: Linear displacement in an inclined system.

It is assumed that the displacement is linear, oil and water are immiscible and the system to be water wet and incompressible. It is also assumed that oil and water saturations at any point in the linear displacement path are uniformly distributed relatively to the thickness. This assumption is defined as the diffuse flow condition. The latter allows the displacement to be considered as one-dimensional. It is accomplished either by high injection rates which allow the effects of capillary and gravity forces to be neglected or by the vertical equilibrium

condition satisfied by low injection rates, large vertical permeability, small reservoir thickness, large density difference between the fluids, large capillary transition zone and low fluid viscosities. (Dake, Fundamentals of Reservoir Engineering 1978)

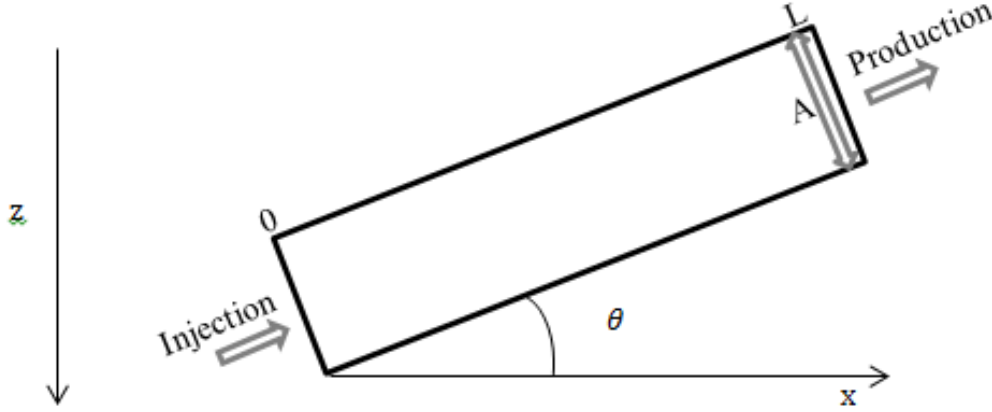


Figure 1: Linear displacement in an inclined system

Based on these assumptions, the flow rate within the system can therefore be described by Darcy's law for two-phase system:

$$q_o = -\frac{A K K_{ro}}{\mu_o} \left(\frac{\partial P_o}{\partial x} + \rho_o g \sin \theta \right) \quad (3.1)$$

$$q_w = -\frac{A K K_{rw}}{\mu_w} \left(\frac{\partial P_w}{\partial x} + \rho_w g \sin \theta \right) \quad (3.2)$$

Adding the flow rate of oil and flow rate of water we get the total flow rate:

$$q_t = -\frac{A K K_{ro}}{\mu_o} \left(\frac{\partial P_o}{\partial x} + \rho_o g \sin \theta \right) - \frac{A K K_{rw}}{\mu_w} \left(\frac{\partial P_w}{\partial x} + \rho_w g \sin \theta \right) \quad (3.3)$$

The mobility of a phase is defined as the ratio of effective permeability to phase viscosity. Therefore, the mobility of oil λ_o , the mobility of water λ_w and the total mobility λ_t can be described as follows:

$$\lambda_o = \frac{K_{ro}}{\mu_o} \quad (3.4)$$

$$\lambda_w = \frac{K_{rw}}{\mu_w} \quad (3.5)$$

$$\lambda_t = \lambda_o + \lambda_w \quad (3.6)$$

The capillary pressure which will be explained in more details in chapter 4 can be expressed as:

$$P_c = P_o - P_w \quad (3.7)$$

Implementing these definitions in equation (3.3) gives:

$$q_t = -\lambda_o A K \left(\frac{\partial(P_c + P_w)}{\partial x} + \rho_o g \sin \theta \right) - \lambda_w A K \left(\frac{\partial P_w}{\partial x} + \rho_w g \sin \theta \right) \quad (3.8)$$

$$q_t = -A K (\lambda_w \rho_w + \lambda_o \rho_o) g \sin \theta - \lambda_t A K \frac{\partial P_w}{\partial x} - \lambda_o A K \frac{\partial P_c}{\partial x} \quad (3.9)$$

Multiplying by $\frac{\lambda_w}{\lambda_t}$ yields:

$$\frac{\lambda_w}{\lambda_t} q_t = -A K \left(\frac{\lambda_w^2}{\lambda_t} \rho_w + \frac{\lambda_w \lambda_o}{\lambda_t} \rho_o \right) g \sin \theta - \lambda_w A K \frac{\partial P_w}{\partial x} - \frac{\lambda_w \lambda_o}{\lambda_t} A K \frac{\partial P_c}{\partial x} \quad (3.10)$$

Rearranging the equation gives:

$$\begin{aligned} \frac{\lambda_w}{\lambda_t} q_t = & -\lambda_w A K \left(\frac{\partial P_w}{\partial x} + \rho_w g \sin \theta \right) + A K \frac{\lambda_w \lambda_o}{\lambda_t} (\rho_w - \rho_o) g \sin \theta \\ & - \frac{\lambda_w \lambda_o}{\lambda_t} A K \frac{\partial P_c}{\partial x} \end{aligned} \quad (3.11)$$

The water flow rate is then:

$$\begin{aligned} q_w = & \underbrace{\frac{\lambda_w}{\lambda_t} q_t}_{\text{viscous forces}} + \underbrace{\frac{\lambda_w \lambda_o}{\lambda_t} A K \frac{\partial P_c}{\partial x}}_{\text{capillary forces}} - \underbrace{A K \frac{\lambda_w \lambda_o}{\lambda_t} (\rho_w - \rho_o) g \sin \theta}_{\text{gravity Forces}} \end{aligned} \quad (3.12)$$

Dividing the flow rate of water by the total flow rate, we get the fractional flow equation:

$$f_w = \frac{q_w}{q_t} = \frac{q_w}{q_w + q_o} = \frac{\lambda_w}{\lambda_t} \left[1 + \frac{A K \lambda_o}{q_t} \left(\frac{\partial P_c}{\partial x} - (\rho_w - \rho_o) g \sin \theta \right) \right] \quad (3.13)$$

In field units, the equation (3.13) can be expressed as:

$$f_w = \frac{\lambda_w}{\lambda_t} \left[1 + \frac{0.001127 A K \lambda_o}{q_t} \left(\frac{\partial P_c}{\partial x} - 0.433 (\rho_w - \rho_o) g \sin \theta \right) \right] \quad (3.14)$$

In order to simplify equation (3.13), we introduce the gravity number N_G which is the ratio of gravity to viscous pressure gradient.

$$N_G(S_w) = \frac{K A \lambda_o (\rho_w - \rho_o) g \sin \theta}{q_t} \quad (3.15)$$

We also define the mobility ratio M which is the ratio of the mobility of the displacing fluid (water) to the mobility of the displaced fluid (oil).

$$M(S_w) = \frac{\lambda_w}{\lambda_o} \quad (3.16)$$

Assuming that the pressure gradients of water and oil are equal, the capillary forces can be neglected and the fractional flow equation is rewritten:

$$f_w = \frac{1 - N_G(S_w)}{1 + \frac{1}{M(S_w)}} \quad (3.17)$$

Finally, assuming that the reservoir is horizontal ($\theta = 0$), i.e. no gravity effect, the fractional flow equation is simplified

$$f_w = \frac{\lambda_w}{\lambda_t} = \frac{1}{1 + \frac{1}{M(S_w)}} \quad (3.18)$$

This equation can be used to determine the water cut at any position of the reservoir but only if the water saturation is known. Buckley and Leverett have therefore derived the frontal advance equation detailed in the next section to determine the water saturation profile at any time.

Equation (3.18) will be used in this chapter to demonstrate Buckley Leverett model. In chapter 4, equation (3.13) will be used to include the effects of gravity and capillary pressure.

3.2 Frontal advance equation

The frontal advance equation is the basic and the simplest equation for the prediction of the behavior of a two phase, immiscible displacement in a linear system. The derivation of the frontal advance equation requires the use of the mass conservation principle. It states that the inflows, outflows and change in storage of mass in a system must be in balance.

We consider a rectangular reservoir with cross-sectional area A , length L and porosity ϕ and we assume that water with density ρ_w illustrated in Figure 1 is flowing through it at a velocity u_w . The mass that enters a volume element of length Δx for a time period of Δt leaves or accumulates in the system.

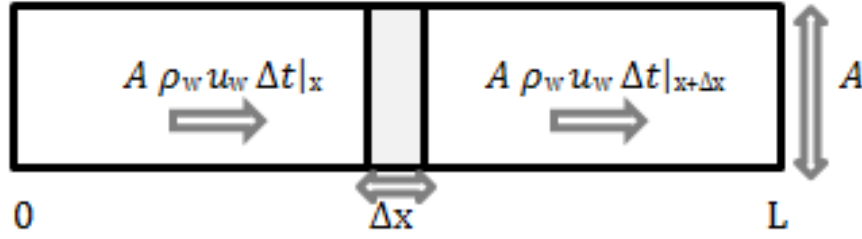


Figure 2: Water flow through a linear differential element

The mass balance for the volume element is expressed as:

$$\begin{array}{c}
 \text{Total Pore Volume} \\
 \underbrace{A \rho_w u_w \Delta t|_x}_{\text{Mass flowing into the element at } x} - \underbrace{A \rho_w u_w \Delta t|_{x+\Delta x}}_{\text{Mass flowing out of the element at } x+\Delta x} = \underbrace{A \Delta x \phi (\rho_w S_w|_{t+\Delta t} - \rho_w S_w|_t)}_{\text{Change of mass inside the element}}
 \end{array} \quad (3.19)$$

Dividing by Δx and Δt , we get:

$$\frac{A \rho_w u_w|_x - A \rho_w u_w|_{x+\Delta x}}{\Delta x} = \phi \frac{(A \rho_w S_w|_{t+\Delta t} - A \rho_w S_w|_t)}{\Delta t} \quad (3.20)$$

For $\Delta x \rightarrow 0$ and $\Delta t \rightarrow 0$

$$- \frac{\partial(A \rho_w u_w)}{\partial x} = \phi \frac{\partial(A \rho_w S_w)}{\partial t} \quad (3.21)$$

We assume that the area A is constant and that the fluid is incompressible (ρ_w is constant).

The continuity equation simplifies to:

$$- \frac{\partial(u_w)}{\partial x} = \phi \frac{\partial(S_w)}{\partial t} \quad (3.22)$$

The negative sign expresses the fact that the water velocity gradient points in the opposite direction to which water accumulates in time; i.e., the rate at which water enters into the reservoir decreases as water saturates it. This means that, when the slice is dry, water enters into it at its fastest rate, declining as water starts occupying its pore spaces.

Using the relation $u_w = f_w u_t$, the previous equation is rewritten:

$$- \frac{\partial(u_t f_w)}{\partial x} = \phi \frac{\partial(S_w)}{\partial t} \quad (3.23)$$

Since $S_w + S_o = 1$ and $\phi \frac{\partial(S_w + S_o)}{\partial t} + \frac{\partial(u_w + u_o)}{\partial x} = 0$, we conclude that $\frac{\partial(u_t)}{\partial x} = 0$.

Hence, the total velocity is constant in space and the continuity equation is reformulated:

$$-u_t \frac{\partial f_w}{\partial x} = \phi \frac{\partial S_w}{\partial t} \quad (3.24)$$

This equation is referred to as the Buckley-Leverett equation. It was solved analytically by Buckley and Leverett. Then, various numerical methods were developed to treat this problem numerically. Both approaches illustrate the saturation profile based on the expression of the rate of advance.

3.3 Buckley-Leverett Solution

3.3.1 Analytical solution

To solve the Buckley-Leverett equation, it is more convenient to use the dimensionless and normalized variables for their simplicity and accuracy. (Hirasaki 2009)

We define the dimensionless position x_D with respect to the system length:

$$x_D = \frac{x}{L} \quad \rightarrow \quad \partial x = L \partial x_D$$

We also define the dimensionless time t_D as the number of movable pore volumes of throughput:

$$t_D = \frac{u_t}{L \phi} t \quad \rightarrow \quad \partial t = \frac{L \phi}{u_t} \partial t_D$$

Using the above equations, we get the dimensionless form of Buckley-Leverett equation as:

$$- \frac{\partial f_w}{\partial x_D} = \frac{\partial S_w}{\partial t_D} \quad (3.25)$$

For simplicity, the equation is rewritten as:

$$- \frac{\partial f}{\partial x} = \frac{\partial S}{\partial t} \quad (3.26)$$

Where S is the water saturation, x is the dimensionless position and t is the dimensionless time verifying $0 \leq x \leq 1$ and $t \geq 0$.

Buckley and Leverett reformulated this equation as shown below to determine an expression for the velocity of any specific water saturation.

$$v = \frac{\partial x}{\partial t} = - \frac{\partial f}{\partial S} \quad (3.27)$$

Equation (3.27) suggests that the rate of advance is directly proportional to the slope of the fractional flow versus the water saturation curve. It also represents the slope of a trajectory of

constant saturation in the (x,t) plane. This can be well elaborated by Figure 3 where each straight line corresponds to a constant saturation ($dS=0$; $S=S_b$). Changes in saturation start at $(0,0)$ since the initial and boundary conditions are assumed to be constant and then they propagate in trajectories of constant saturation. These changes are referred to as waves (Hirasaki 2009) .

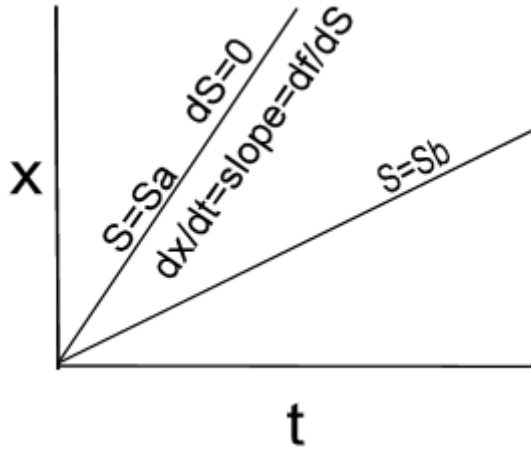


Figure 3: Velocity corresponding to a constant saturation ($dS=0$ or $S=S_b$) at (x,t) plane

Equation (3.27) will also be used later to generate the saturation profile and the fractional flow curve. But first, the fractional flow equation should be expressed as a function of the water saturation S . This can be done by establishing a relationship between the relative permeability and the water saturation.

Various correlations have been developed to relate the relative permeability to the water saturation. The Modified Brooks-Corey model, also called the power law model will be discussed in this thesis. The MBC equations (H.M. Goda 2004) can be expressed as:

$$k_{rw} = K_{rw@Sor} (S_{wn})^{nw} \quad (3.28)$$

$$k_{ro} = K_{ro@Swc} (1 - S_{wn})^{no} \quad (3.29)$$

$$S_{wn} = \frac{S_w - S_{wi}}{1 - S_{wi} - S_{or}} \quad (3.30)$$

Where $K_{rw@Sor}$ is the relative permeability of water at the residual oil saturation, $K_{ro@Swc}$ is the relative permeability of oil at the connate water saturation, nw is the Corey water exponent, no is the Corey oil exponent, S_{wi} is the initial water saturation and S_{or} is the residual oil saturation. The exponents no and nw range from 1 to 6.

Figure 4 shows Corey relative permeabilities for $no = 2$, $nw = 2$, $K_{rw@Sor} = 0.3$, $K_{ro@Swc} = 0.7$, $S_{wi} = 0.2$ and $S_{or} = 0.25$:

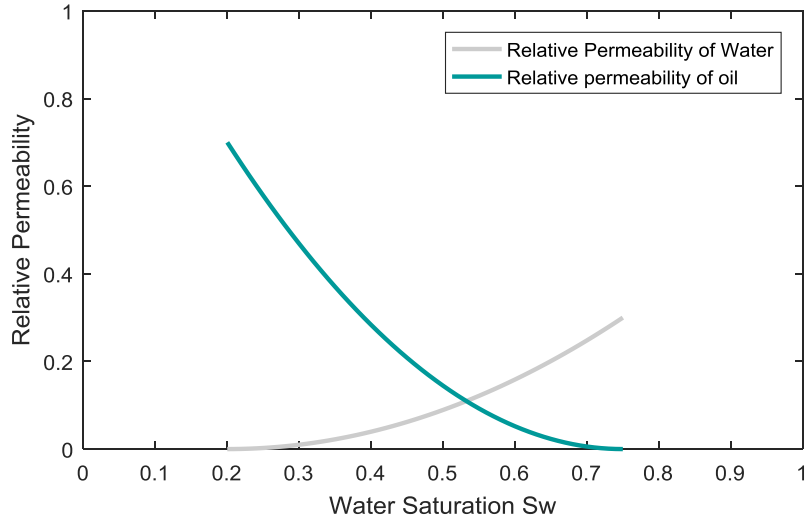


Figure 4: Corey Relative Permeability

If we substitute the Corey relative permeability equations in the fractional flow equation, we get:

$$f_w = \frac{\lambda_w}{\lambda_t} = \frac{K_{rw}}{K_{rw} + k_{ro} \frac{\mu_w}{\mu_o}} = \frac{K_{rw@Sor} (S_{wn})^{nw}}{K_{rw@Sor} (S_{wn})^{nw} + \frac{\mu_w}{\mu_o} K_{ro@Swc} (1 - S_{wn})^{no}} \quad (3.31)$$

As can be seen, the fractional flow equation is only dependent on the water saturation. Hence, the fractional flow curve can be easily generated by Matlab code as explained in appendix B.

For relative permeability just introduced in Figure 4 and $\frac{\mu_w}{\mu_o} = 0.5$, the fractional flow curve is as follows:

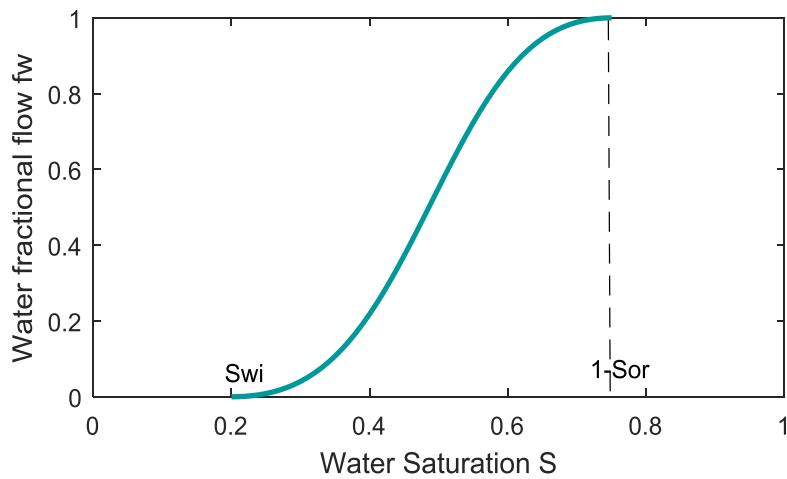


Figure 5: Fractional Flow curve

Next step is the construction of the saturation profile. To do that analytically, we use the dimensionless position as function of the water saturation. For that purpose, we write the following equation for saturation change which is dependent on time and position:

$$dS_w = \frac{\partial S_w}{\partial x} dx + \frac{\partial S_w}{\partial t} dt \quad (3.32)$$

Since during the displacement process, the fluid front is assumed of constant saturation, equation (3.32) becomes:

$$0 = \frac{\partial S_w}{\partial x} dx + \frac{\partial S_w}{\partial t} dt \quad (3.33)$$

Substituting in equation (3.27) yields:

$$\frac{dx}{dt} = \frac{df}{dS} \quad (3.34)$$

Integrating in time

$$\int \frac{dx}{dt} dt = \int \frac{df}{dS} dt \quad (3.35)$$

This yields to the following equation that is used for the construction of the saturation profile after determining the derivative of fractional flow.

$$x = t \left(\frac{\partial f}{\partial S} \right) \quad (3.36)$$

Therefore, we calculate the derivative of the fractional flow with respect to the water saturation using equation 3.28. The equation of the dimensionless position is therefore expressed as:

$$x = t \frac{M K_{rw@Sor} K_{ro@Swc} (1 - S_{wn})^{no-1} (S_{wn})^{nw-1} (nw (1 - S_{wn}) + no S_{wn})}{(K_{rw@Sor} (S_{wn})^{nw} + \frac{\mu_w}{\mu_o} K_{ro@Swc} (1 - S_{wn})^{no})^2} \quad (3.37)$$

The derivative of the fractional flow curve and the saturation profile generated by the MATLAB code detailed in appendix B have the shape shown in Figure 6: Derivative of Fractional Flow and Figure 7 respectively (elapsed time = 0.5).

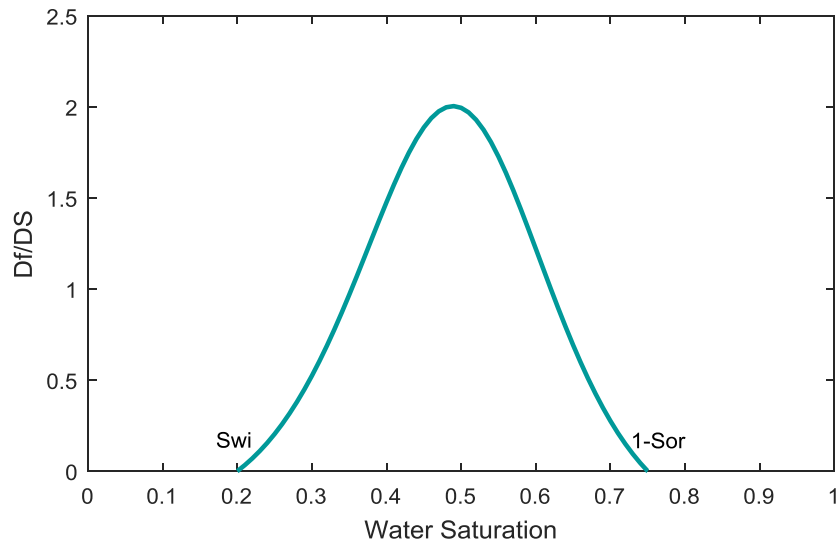


Figure 6: Derivative of Fractional Flow

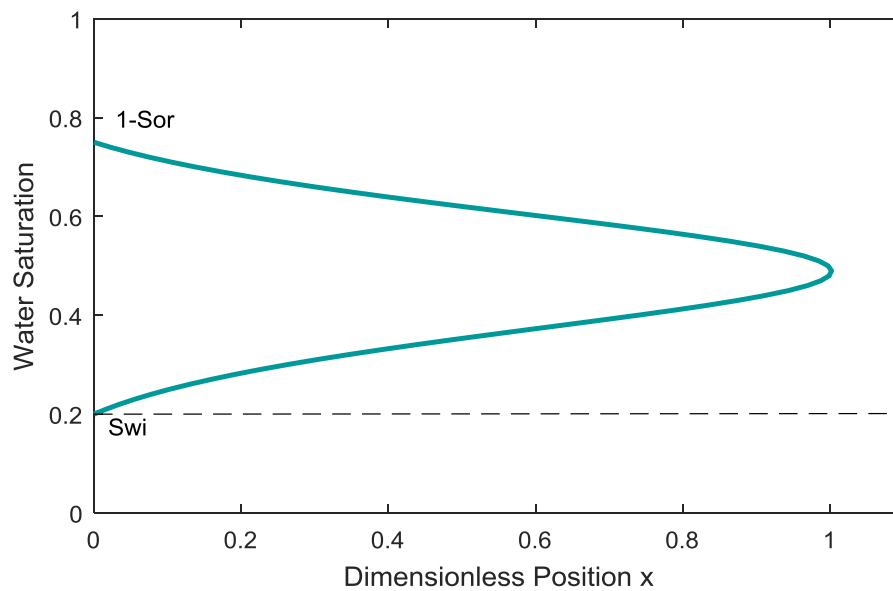


Figure 7: Saturation Profile, Unphysical Solution

The same data used to construct the fractional flow curve was also used to generate these curves. Figure 8 shows the saturation profile for different values of the elapsed time (0.05, 0.1, 0.15, 0.2, 0.25, 0.3, 0.35, 0.4, 0.45, 0.5, 0.55, 0.6).

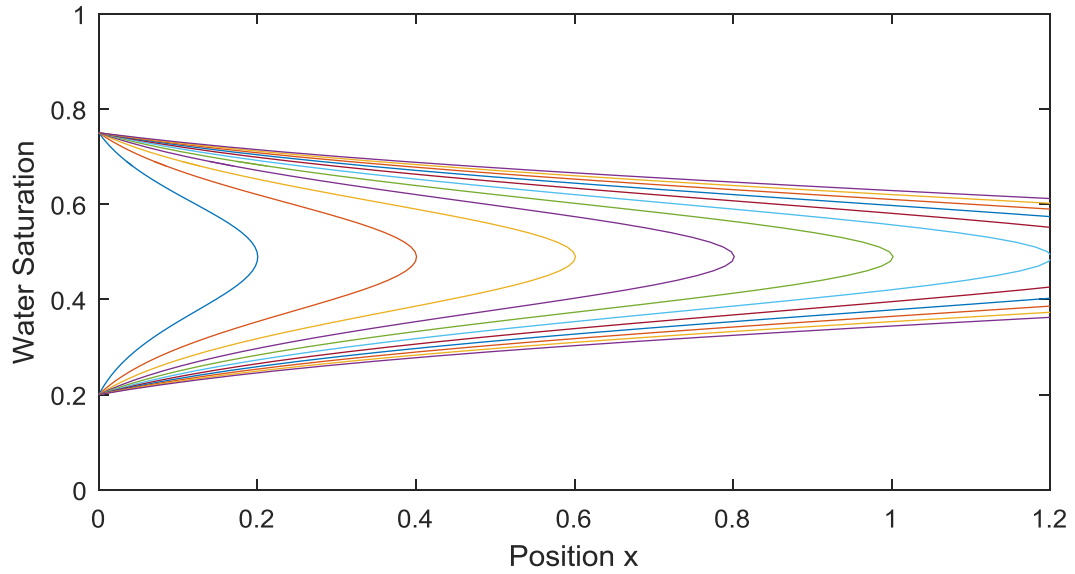


Figure 8: Saturation Profile at different times

It can be seen from the derivative of fractional flow curve that the velocity has a maximum point. This implies that at the same velocity, low and high saturations can travel at the same velocity, which is physically absurd. This absurdity is confirmed by the saturation profile. The latter suggests that it is possible to have multiple saturation values at the same position in a linear system. This is also unrealistic.

This problem is conquered by assuming a saturation discontinuity or a shock front.

3.3.2 Shock front

3.3.2.1 Material Balance

The idea of the shock front is best explained by waves. The wave is an oscillation propagated through a medium or space. We distinguish between different types of waves. (1) The spreading wave is a wave that becomes more distributed upon propagation. The slope $\frac{dS}{dx}$ decreases over time. (2) The indifferent wave maintains the same relative position upon propagation. The slope $\frac{dS}{dx}$ is constant. (3) The self-sharpening wave is a wave that becomes less diffuse upon propagation. The slope $\frac{dS}{dx}$ increases over time. The shock wave results from the self-sharpening wave. The slope $\frac{dS}{dx}$ is undefined.

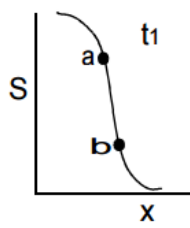


Figure 9: Spreading Wave

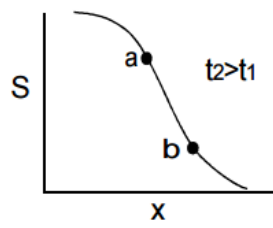


Figure 10: Indifferent wave

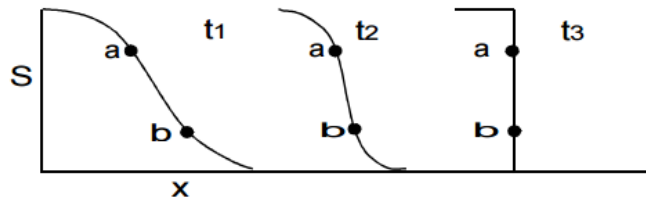


Figure 11: Self-sharpening wave resulting in a shock wave

In Buckley-Leverett problem, there is more than one type of waves. Slow and fast waves are generated at the same time. Commonly, faster waves are ahead of the slower waves. But, if slower waves are preceding, faster waves come past them. This results in a shock front illustrated in Figure 12.

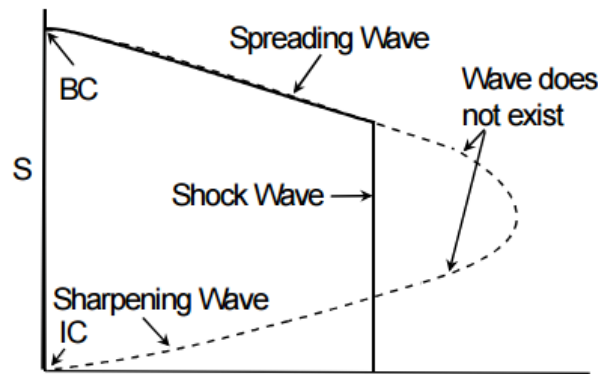


Figure 12: The Buckley-Leverett wave

It is then appropriate to assume a shock front in Buckley-Leverett problem. But the saturation of the shock front should be determined. This can be performed by Welge's method or by the material balance technique.

The material balance technique suggests that the area denoted A1 must be equal to the area denoted A2 as shown in Figure 13. The line separating the two areas represents the shock front saturation discontinuity.

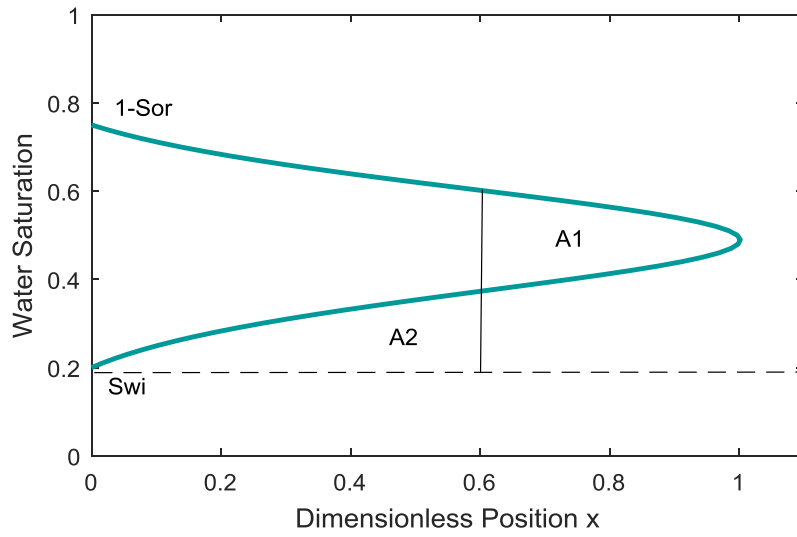


Figure 13: Saturation Profile, Physical Solution

From Figure 13, we can express the areas A1 and A2:

$$A1 = \int_{S_{wi}}^{1-S_{or}} t f'(S) dS = t [f(1 - S_{or}) - f(S_{wi})] \quad (3.38)$$

$$\begin{aligned} A2 &= t f'(S_{wf})(S_{wf} - S_{wi}) \\ &\quad + \int_{S_{wf}}^{1-S_{or}} t f'(S) dS \\ &= t f'(S_{wf})(S_{wf} - S_{wi}) + t[f(1 - S_{or}) - f(S_{wf})] \end{aligned} \quad (3.39)$$

Applying the mass conservation yields to:

$$f'(S_{wf}) = \left(\frac{\partial f}{\partial S} \right)_{S_{wf}} = \frac{f(S_{wf}) - f(S_{wi})}{S_{wf} - S_{wi}} \quad (3.40)$$

If this equation is verified, then the areas A1 and A2 are equal and we get the corrected saturation profile.

3.3.2.2 Welge's method

Another method for the determination of the shock front saturation involving the average water saturation was developed by Welge (Welge 1952). The average water saturation illustrated in Figure 14 is determined by the integration of the saturation distribution over the distance from the injection line to the position of the front.

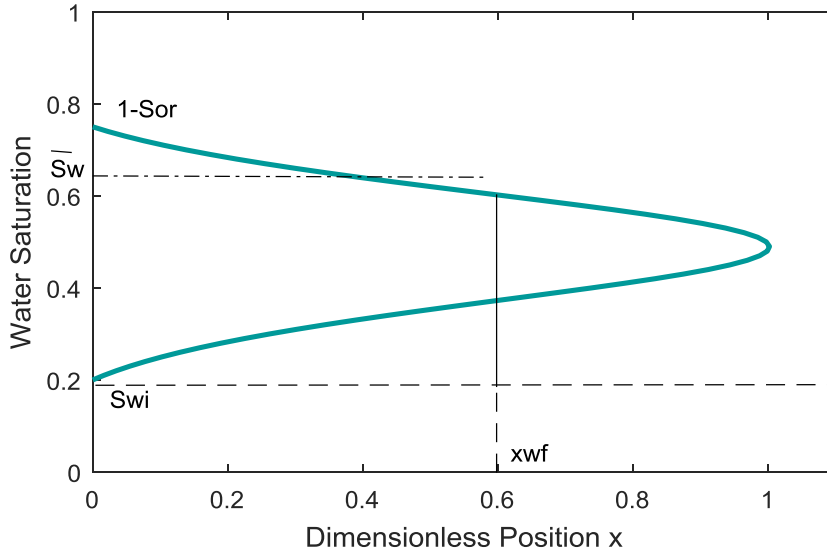


Figure 14: Illustration of the average water saturation

Thus, the average saturation is expressed as:

$$\bar{S}_w = \frac{\int_0^{x_{wf}} S_w dx}{\int_0^{x_{wf}} dx} = S_{wf} + \frac{1 - f_{wf}}{\left(\frac{\partial f_w}{\partial S_w}\right)_{S_{wf}}} \quad (3.41)$$

Furthermore, the material balance for the injected water is applied:

$$W_i = A \phi x_{wf} (\bar{S}_w - S_{wi}) \quad (3.42)$$

And the Buckley-Leverett equation is evaluated for the shock front saturation.

$$x_{wf} = \frac{W_i}{A\phi} \left(\frac{\partial f_w}{\partial S_w}\right)_{S_{wf}} \quad (3.43)$$

Combining the above equations yields to:

$$\bar{S}_w = S_{wi} + \frac{1}{\left(\frac{\partial f_w}{\partial S_w}\right)_{S_{wf}}} \quad (3.44)$$

Consequently,

$$\left(\frac{\partial f_w}{\partial S_w}\right)_{S_{wf}} = \frac{1 - f_{wf}}{\bar{S}_w - S_{wf}} = \frac{1}{\bar{S}_w - S_{wi}} \quad (3.45)$$

According to this equation, the saturation at the displacing front can be determined by drawing a line from the initial water saturation and tangent to the fractional flow curve. The point of tangency represents the water saturation at the front. The intersection between the tangent line illustrated in Figure 15 and the line $f_w = 1$ represents the average water saturation.

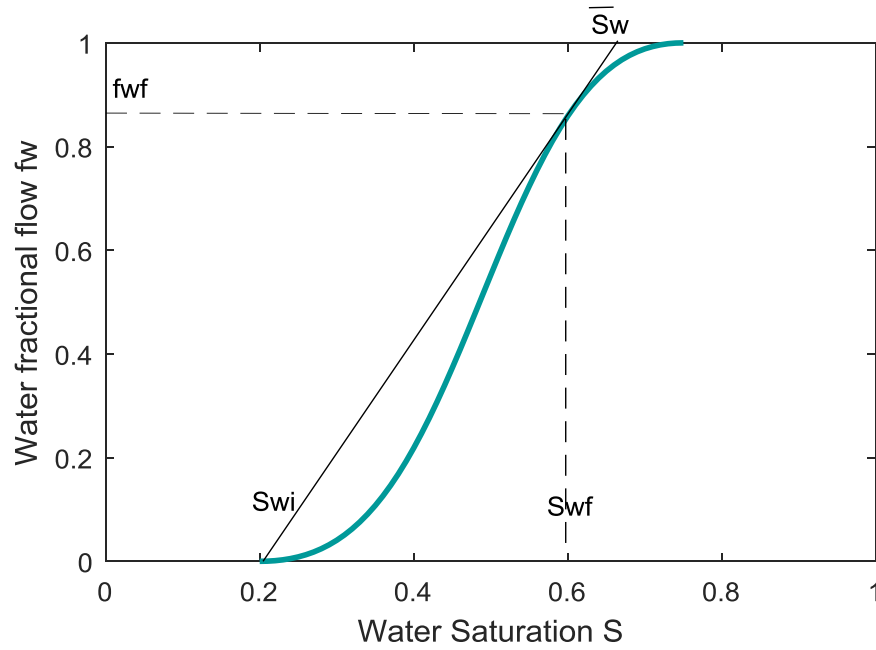


Figure 15: Graphical Determination of Front Saturation

It is important to note that the Buckley-Leverett theory can only be used behind the front. In other words, the fractional flow curve is used in the range where it is permitted to neglect the capillary pressure effects and that is when $S_{wf} < S_w < 1 - S_{or}$.

After assuming a shock front, we obtain the physical solution of the saturation profile at various time steps illustrated in Figure 16 using provided code.

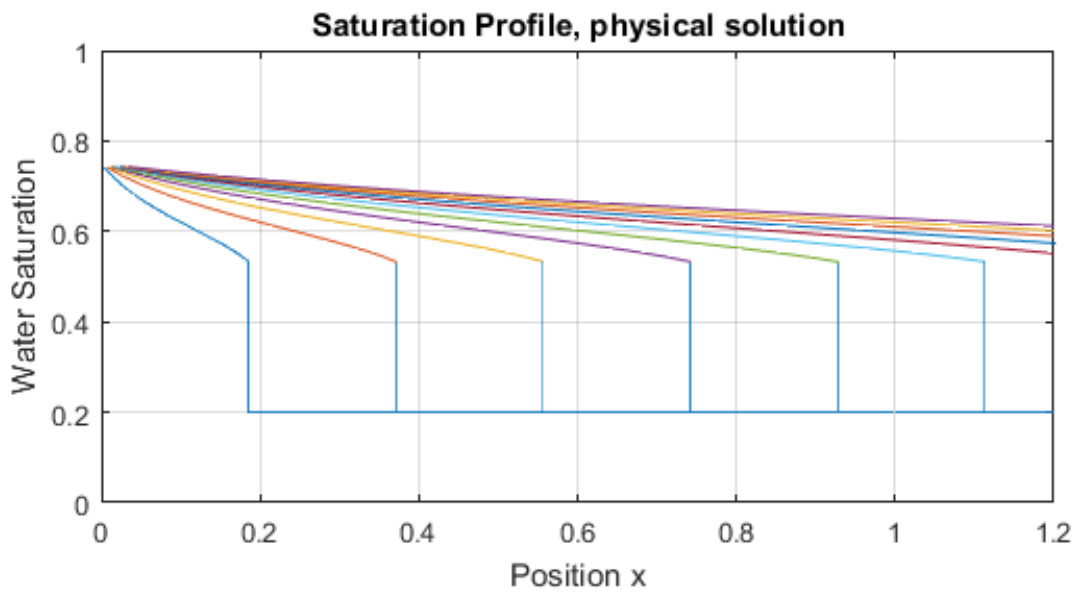


Figure 16: Saturation Profile, Physical solution

3.3.3 Numerical Solution

To simulate Buckley-Leverett problem numerically, here we focus on 1D geometry.

$$-\frac{\partial f_w}{\partial x} = \frac{\partial S_w}{\partial t} \quad (3.46)$$

First, the geometry should be discretized, herein we opt for the finite difference methods. So, the geological model is turned into a discrete system by subdividing the x-axis into N grid blocks as illustrated in *Figure 17* and the time coordinate into discrete time steps. This is referred to as spatial and time discretization and we get a block centered grid configuration. (Kazemi 2009)

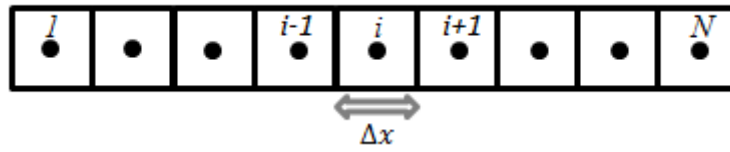


Figure 17: Dimensional core space discretization

Second, the first order time derivative and the first order space derivative are approximated by Taylor series approximation. The expansion can be forwards or backwards.

Expanding the space derivative backwards for constant time gives:

$$f_w(x - \Delta x, t) = f_w(x, t) + \frac{-\Delta x}{1!} f_w'(x, t) + \frac{(-\Delta x)^2}{2!} f_w''(x, t) + \frac{(-\Delta x)^3}{3!} f_w'''(x, t) + \dots \quad (3.47)$$

Rearranging the equation (3.47) and solving for f_w' yields to:

$$f_w'(x, t) = -\frac{f_w(x - \Delta x, t) - f_w(x, t)}{\Delta x} + \frac{\Delta x}{2} f_w''(x, t) + \dots \quad (3.48)$$

Rewriting the equation using the index i introduced in Figure 16 results in:

$$\left(\frac{\partial f_w}{\partial x}\right)_i^t = -\frac{f_w^t_{i-1} - f_w^t_i}{\Delta x} + O(\Delta x) \quad (3.49)$$

Then, the saturation function is expanded with respect to time forwards for a constant position x :

$$S_w(x, t + \Delta t) = S_w(x, t) + \frac{\Delta t}{1!} S_w'(x, t) + \frac{(\Delta t)^2}{2!} S_w''(x, t) + \frac{(\Delta t)^3}{3!} S_w'''(x, t) + \dots \quad (3.50)$$

Solving for the first derivative with respect to time, we get:

$$S_w'(x, t) = \frac{S_w(x, t + \Delta t) - S_w(x, t)}{\Delta t} + \frac{\Delta t}{2} S_w''(x, t) + \dots \quad (3.51)$$

Rewriting the first derivative with employing the index system yields to:

$$\left(\frac{\partial S_w}{\partial t}\right)_i^t = \frac{S_{w,i}^{t+\Delta t} - S_{w,i}^t}{\Delta t} + O(\Delta t) \quad (3.52)$$

Third, the expanded time and space derivatives are replaced in Buckley-Leverett equation. Depending on the time discretization scheme we can get explicit or implicit formulation. In this thesis an explicit discretization is selected.

Explicit methods determine the state of a system at $t + \Delta t$ using the state of a system at the current time t . Thus, the equations (3.49) and (3.52) at time level t are substituted in Buckley-Leverett equation.

$$\frac{f_{w,i-1}^t - f_{w,i}^t}{\Delta x} = \frac{S_{w,i}^{t+\Delta t} - S_{w,i}^t}{\Delta t} \quad (3.53)$$

Then, we solve for $S_{w,i}^{t+\Delta t}$:

$$S_{w,i}^{t+\Delta t} = \frac{\Delta t}{\Delta x} (f_{w,i-1}^t - f_{w,i}^t) + S_{w,i}^t \quad (3.54)$$

The explicit upwind discretization is only stable when the Courant–Friedrichs–Levy (CFL) condition is verified. It is a necessary condition for convergence when using the finite difference method to solve the partial differential equations. The time step should be lower than a specific value to avoid unrealistic results or errors. The condition that should be satisfied is $\frac{\Delta t}{\Delta x} \leq 1$.

Lastly, the equations are solved using computer codes detailed in appendix C leading to Figure 18.

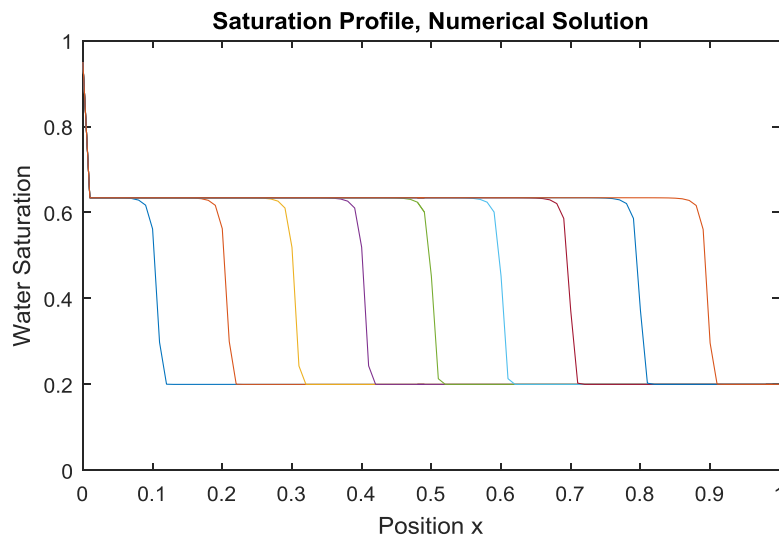


Figure 18: Saturation Profile, Numerical Solution

3.3.4 Comparison of the analytical and the numerical solutions

In order to provide a reliable comparison, the same reservoir condition and physical properties were utilized for the analytical and numerical solutions ($no = 2$, $n_w = 2$, $K_{rw@Sor} = 1$, $K_{ro@Swc} = 1$, $S_{wi} = 0$, $S_{or} = 0$ and $\frac{\mu_w}{\mu_o} = 0.9$). Figure 19 shows the saturation profiles for both solutions.

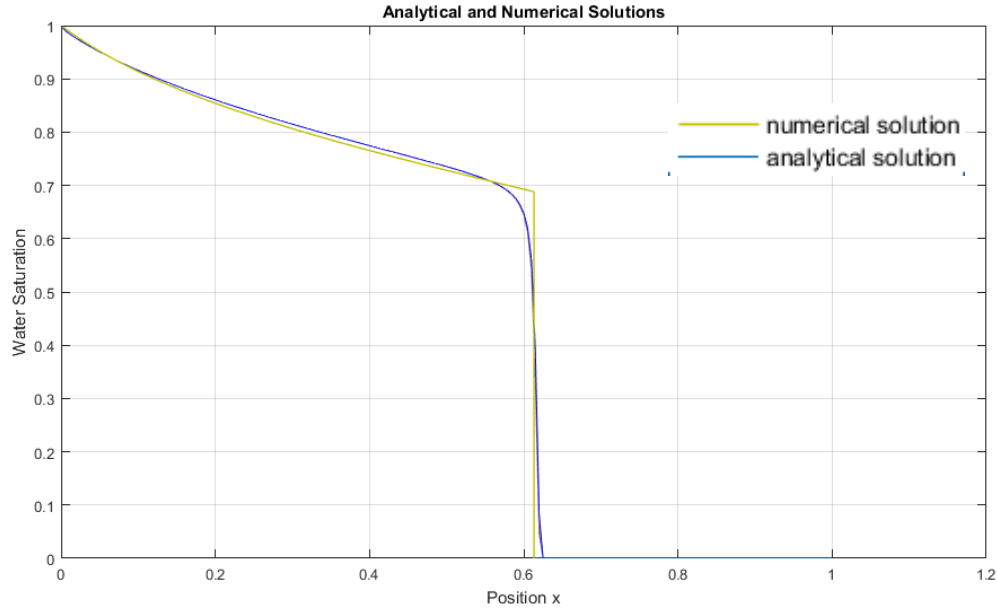


Figure 19: Comparison between the analytical and numerical solutions

It can be seen from Figure 19 that the analytical and the numerical solutions are comparable. However, a smearing of the displacement front in the numerically solved solution is present. This can be improved by refining the grid spacing.

In addition, there is a limitation to the explicit discretization which consists of the stability criterion of Courant–Friedrichs–Levy (CFL). To achieve meaningful solutions from the reservoir simulation, it is necessary to maintain computational stability. This is overcome by selecting an appropriate value for Δt . It is also important to note that other numerical methods which do not require a stability criterion can be implemented. One such a method is the implicit solution. The latter evaluates some or all of the terms with involving both the current state of the system and the later one. (Abidullah ARABZAI 2013)

Chapter 4

Generalized Buckley-Leverett Equation

The effects of Gravity and capillary pressure will be investigated separately to see the influence of each one on the waterflooding process.

4.1 Gravity Effect

The petroleum reservoirs can either be horizontal as discussed in chapter 3 or tilted. The system introduced in Figure 1 will be considered in this section. It is characterized by an angle θ . The latter characterizes the presence of a gravity component which has an effect on the displacement process. It either retards or aids the displacement.

To study the effect of gravity, recall the fractional flow equation below. Herein, the angle is not negligible and therefore the gravity term's value N_G should be observed.

$$f_w = \frac{1 - N_G(S_w)}{1 + \frac{1}{M(S_w)}}$$

where

$$N_G(S_w) = \frac{K A \lambda_o (\rho_w - \rho_o) g \sin \theta}{q_t}$$

The same steps as in the previous chapter are followed to plot the fractional flow curve: the modified Brooks Corey model is employed in the fractional flow equation to relate the relative permeability to the water saturation.

$$\begin{aligned}
 f_w &= \frac{1 - N_G(S_w)}{1 + \frac{1}{M(S_w)}} \\
 &= \frac{K_{rw@Sor} (S_{wn})^{nw}}{K_{rw@Sor} (S_{wn})^{nw} + \frac{\mu_w}{\mu_o} K_{ro@Swc} (1 - S_{wn})^{no}} (1 - N_G(S_w)) \quad (4.1)
 \end{aligned}$$

$$f_w = \frac{1 - N_G(S_w)}{1 + \frac{1}{M(S_w)}} = \frac{K_{rw@Sor} (S_{wn})^{nw}}{K_{rw@Sor} (S_{wn})^{nw} + \frac{\mu_w}{\mu_o} K_{ro@Swc} (1 - S_{wn})^{no}} (1 - N_G(S_w)) \quad (4.2)$$

Since $N_G(S_w)$ depends on the saturation, we introduce a gravity number N_G° to see the effect of the dip angle, such as $N_G(S_w) = K_{ro} N_G^\circ$. N_G° is a constant which depends on the total velocity, the gravitational constant, the dip angle, the oil viscosity and the density difference. It is represented by this formula:

$$N_G^\circ = \frac{K A (\rho_w - \rho_o) g \sin \theta}{\mu_o q_t} \quad (4.3)$$

To inspect the effect of the gravity number, the dip angle is varied between -20° and 20° leading to the results in Figure 20.

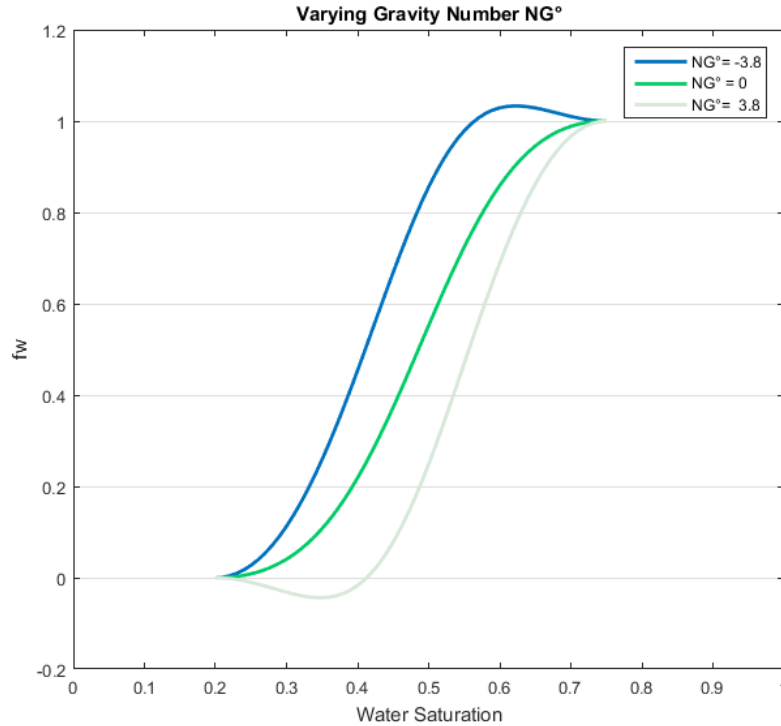


Figure 20: Effect of changing gravity number on the fractional flow curve

The code and the parameters used are detailed in Appendix D.

It can be seen from Figure 20 that for a one-dimensional multiphase flow (Hirasaki 2009) the value of f_w decreases for positive gravity numbers. That means for a given saturation, a displacement of oil upwards declines the fractional flow of water leading to a stabilized displacement. However, the value of f_w increases for negative gravity numbers. The latter implies that for a given saturation a displacement of oil downwards increases the fractional flow of water.

4.2 Capillary Pressure Effect

The capillary forces in a petroleum system are dependent on the effects of the surface and interfacial tensions of the rock and fluids, the pore size and geometry, and the wetting characteristics of the system. They occur when two different fluids (e.g. water and oil) are simultaneously present leading to a differential pressure at the interface separating the two fluids. The pressure difference is referred to as capillary pressure.

In a porous medium, the capillary pressure can be obtained by subtracting the pressure of the non-wetting phase (oil) from the pressure of the wetting phase (water) as expressed below:

$$P_c = P_{nw} - P_w = P_o - P_w \quad (4.4)$$

It can be concluded from this formula that to have a reservoir saturated with oil, it is necessary that the pressure of oil is higher than that of water as the capillary forces act against the non-wetting fluid. (Ahmed 2001)

In the following, the capillary pressure effect will be investigated by extending the basic Buckley-Leverett equation and solving it numerically. (Helvig 2013)

From one hand, recall the equations

$$u_o = -\lambda_o \frac{\partial P_o}{\partial x} \quad (4.5) \quad \text{and} \quad u_w = -\lambda_w \frac{\partial P_w}{\partial x} \quad (4.6)$$

Total velocity, u_t , can be derived by combining Darcy's velocity and capillary pressure as:

$$u_t = u_o + u_w = -\left(\lambda_o \frac{\partial P_o}{\partial x} + \lambda_w \frac{\partial P_w}{\partial x} \right) \quad (4.7)$$

$$= -\left(\lambda_o \frac{\partial P_o}{\partial x} - \lambda_w \frac{\partial P_c}{\partial x} + \lambda_w \frac{\partial P_o}{\partial x} \right) \quad (4.8)$$

$$u_t = \lambda_w \frac{\partial P_c}{\partial x} - \lambda_t \frac{\partial P_o}{\partial x} \quad (4.9)$$

We know from chapter 3 that $\frac{\partial}{\partial x} u_t = 0$,

$$\frac{\partial}{\partial x} (\lambda_w \frac{\partial P_c}{\partial x} - \lambda_t \frac{\partial P_o}{\partial x}) = 0 \quad (4.10)$$

$$\frac{\partial P_o}{\partial x} = \frac{\lambda_w}{\lambda_t} \frac{\partial P_c}{\partial x} - \frac{u_t}{\lambda_t} \quad (4.11)$$

From the other hand,

$$u_w = -\lambda_w \frac{\partial P_w}{\partial x} = -\lambda_w (\frac{\partial P_o}{\partial x} - \frac{\partial P_c}{\partial x}) \quad (4.12)$$

Inserting equation (4.10) in the following equation $-\frac{\partial(u_w)}{\partial x} = \phi \frac{\partial(S_w)}{\partial t}$ yields to

$$\frac{\partial}{\partial x} (\lambda_w (\frac{\partial P_o}{\partial x} - \frac{\partial P_c}{\partial x})) = \phi \frac{\partial(S_w)}{\partial t} \quad (4.13)$$

Using the previous derivation (4.11) gives the following

$$\frac{\partial}{\partial x} (\lambda_w (\frac{\lambda_w}{\lambda_t} \frac{\partial P_c}{\partial x} - \frac{u_t}{\lambda_t})) - \frac{\partial}{\partial x} (\lambda_w \frac{\partial P_c}{\partial x}) = \phi \frac{\partial(S_w)}{\partial t} \quad (4.14)$$

Finally, since $f_w = \frac{\lambda_w}{\lambda_t}$ and $\lambda_w f_w - \lambda_w = -\lambda_o f_w$, we can get the following equation

$$\frac{\partial}{\partial x} (-\lambda_o f_w \frac{\partial P_c}{\partial x}) = \phi \frac{\partial(S_w)}{\partial t} + \frac{\partial}{\partial x} f_w u_t \quad (4.15)$$

Equation (4.15) is a diffusion equation describing the variation in space and time of a physical property.

4.2.1 Numerical solution

Dimensionless variables are used to simplify the obtained equation. Therefore, the dimensionless position and the dimensionless time from chapter 3 are utilized and other dimensionless variables are introduced as follows:

We define dimensionless capillary pressure as the ratio of capillary pressure to the reference capillary pressure, which is dependent on the capillary pressure correlation selected:

$$P_{c,D} = \frac{P_c}{P_{c,r}} \quad \rightarrow \quad \partial P_c = P_{c,r} \partial P_{c,D}$$

We also introduce dimensionless oil viscosity, which is the ratio of oil viscosity to the reference viscosity:

$$\mu_{oD} = \frac{\mu_o}{\mu_r} \quad \rightarrow \quad \lambda_o = \frac{K_{ro}}{\mu_r \mu_{oD}}$$

Using the above equations, we get the dimensionless form of the generalized Buckley-Leverett equation:

$$\frac{P_{c,r}}{L \mu_r u_t} \frac{\partial}{\partial x_D} \left(-\frac{K_{ro}}{\mu_{oD}} f_w \frac{\partial P_{c,D}}{\partial x_D} \right) = \frac{\partial(S_w)}{\partial t_D} + \frac{\partial}{\partial x_D} f_w \quad (4.16)$$

For simplicity, the equation is rewritten as:

$$\frac{P_{c,r}}{L \mu_r u_t} \frac{\partial}{\partial x} \left(-\frac{K_{ro}}{\mu_{oD}} f \frac{\partial P_c}{\partial x} \right) = \frac{\partial(S)}{\partial t} + \frac{\partial}{\partial x} f \quad (4.17)$$

Where S is the water saturation, x is the dimensionless position, t is the dimensionless time and P_c is the dimensionless capillary pressure.

To proceed, we define the following parameters:

- The dimensionless characteristic number ε is the ratio of the reference capillary pressure to the porous media length, the reference oil viscosity and the injection rate. It will demonstrate the effect of capillarity on the displacement process.

$$\varepsilon = \frac{P_{c,r}}{L u_r u_t}$$

- The diffusion coefficient $a(S)$ is the ratio of relative permeability of oil and the fractional flow equation to the dimensionless viscosity. (Helvig 2013)

$$a(S) = -\frac{K_{ro}}{\mu_{oD}} f$$

Implementing these parameters in equation (4.17) yields to:

$$\frac{\partial S}{\partial t} + \frac{\partial f(S)}{\partial x} = \varepsilon \frac{\partial}{\partial x} \left(a(S) \frac{\partial P_c}{\partial x} \right) \quad (4.18)$$

This equation represents the Buckley Leverett equation including the effects of capillary pressure.

It is not possible to solve it analytically (P. K. Helvig 2011). Therefore, the problem will be solved numerically using an explicit discretization. First, the geometry is turned into a discrete system by subdividing the x -axis into K grid blocks with length Δx of $\frac{1}{K}$ and the time axis into N discrete steps with length Δt of $\frac{1}{N}$.

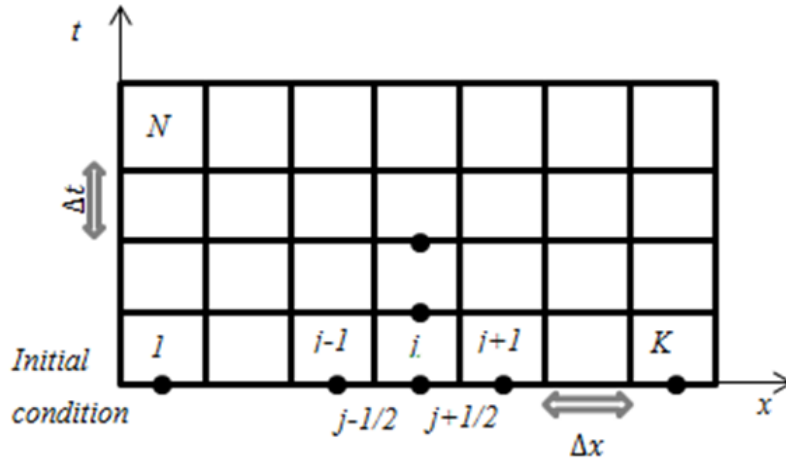


Figure 21: Space and time discretization

The steps followed to get discrete formulation of problem are similar to the methodology utilized for the explicit formulation of the simple equation of Buckley Leverett. The explicit form of equation is obtained as:

$$\begin{aligned} \frac{S_j^{n+1} - S_j^n}{\Delta t} + \frac{1}{\Delta x} (F_{j+1/2}^n - F_{j-1/2}^n) \\ = \frac{\varepsilon}{\Delta x} \left(a_{j+1/2}^n \frac{P_{cj+1}^n - P_{cj}^n}{\Delta x} - a_{j-1/2}^n \frac{P_{cj}^n - P_{cj-1}^n}{\Delta x} \right) \end{aligned} \quad (4.19)$$

Where $j = 2, \dots, K - 1$

Then, we solve for S_j^{n+1}

$$\begin{aligned} S_j^{n+1} = S_j^n - \frac{\Delta t}{\Delta x} (F_{j+1/2}^n - F_{j-1/2}^n) \\ + \frac{\varepsilon \Delta t}{\Delta x} \left(a_{j+1/2}^n \frac{P_{cj+1}^n - P_{cj}^n}{\Delta x} - a_{j-1/2}^n \frac{P_{cj}^n - P_{cj-1}^n}{\Delta x} \right) \end{aligned} \quad (4.20)$$

Where $a_{j\pm 1/2}^n = \frac{1}{2} (a_{j\pm 1}^n + a_j^n)$

The function F called numerical flux and representing an approximation of f , is formulated as follows.

$$F_{j+1/2}^n = \frac{1}{2} (F(S_j^n) + F(S_{j+1}^n)) - \frac{1}{2} D (S_{j+1}^n - S_j^n) \quad (4.21)$$

D is a value that satisfies $D \geq \max[f']$

The formulas above are valid for j from 2 to $K-1$. The next step is the discretization at the boundaries corresponding to $j=1$ (Equation 4.16) and $j=K$ (Equation 4.17).

$$\frac{S_1^{n+1} - S_1^n}{\Delta t} + \frac{1}{\Delta x} (F_{1+1/2}^n - F_{1/2}^n) = \frac{\varepsilon}{\Delta x} \left(a_{1+1/2}^n \frac{P_{c2}^n - P_{c1}^n}{\Delta x} - a_{1/2}^n \frac{P_{c1}^n - P_{c0}^n}{\Delta x/2} \right) \quad (4.22)$$

Where $P_{c0}^n = P_c(S = 1)^n$, $a_{1/2}^n = a_1^n$, $F_{1/2}^n = F^n(S = 1)$

$$\begin{aligned} \frac{S_K^{n+1} - S_K^n}{\Delta t} + \frac{1}{\Delta x} (F_{K+1/2}^n - F_{K-1/2}^n) \\ = \frac{\varepsilon}{\Delta x} \left(a_{K+1/2}^n \frac{P_{cK+1}^n - P_{cK}^n}{\Delta x/2} - a_{K-1/2}^n \frac{P_{cK}^n - P_{cK-1}^n}{\Delta x} \right) \end{aligned} \quad (4.23)$$

Where $P_{cK+1}^n = P_c(S_K)^n$, $a_{K+1/2}^n = a^n(S_K)$, $F_{K+1/2}^n = F^n(S_K)$

It is important to note that the Courant-Friedrich-Levy condition should be satisfied since herein we opted for an explicit discretization ($\frac{\Delta t}{\Delta x} \max[f'] \leq 1$ and $\frac{\Delta t}{\Delta x^2} \max[a(S) * P_c'] \varepsilon \leq 1$)

There are multiple capillary pressure correlations depending on the phases present that can be used to perform the simulation.

- Thomeer suggested a model to describe mercury-injection pressure data (Thomeer 1960)
- Brooks and Corey proposed a model for capillary pressure during primary drainage of oil from an oil saturated porous medium in the presence of gas invasion (Brooks 1964)
- Bentsen and Anli created a model for capillary pressure for a primary drainage process of a system initially saturated by water which is later on invaded by oil (Bentsen 1976)

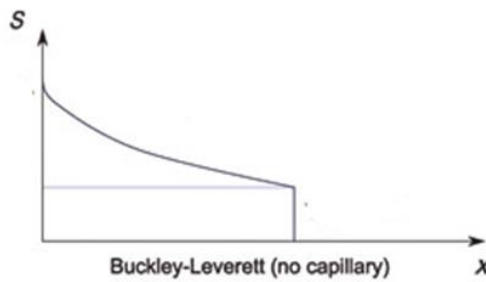


Figure 22: Saturation Profile with Capillary Pressure Effect

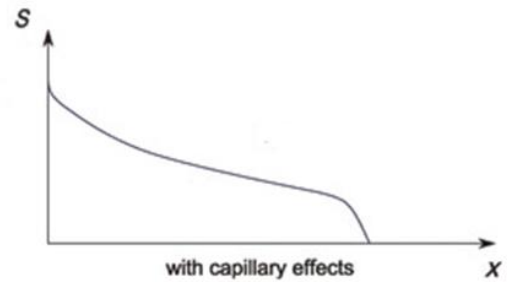


Figure 23: Saturation Profile without Capillary Pressure

If we compare Figure 22 and Figure 23, we can affirm that the effect of capillary pressure is noticeable at the shock front. A smearing out of the solution accounting for the capillary pressure can be observed. The smearing effect is due to the term ε and the higher ε , the more the displacement front tends to be smeared out. Specifically, reducing the injection rate,

reference viscosity and porous media length leads to a smoother curve. The results are also dependent on the capillary pressure correlation used.

Chapter 5

Conclusion

5.1 Summary

In the body of this thesis, waterflooding in a reservoir was explained through Buckley-Leverett theory which is known for providing an estimation for the water saturation in the displacement process.

First, a one dimensional, incompressible and multiphase reservoir was considered. The fractional flow equation and the frontal advance equation being the basis of Buckley-Leverett theory were derived. Then, an analytical solution was implemented. For that purpose, dimensionless variables were introduced. The solution obtained was unrealistic since the derivative of fractional flow showed a maximum value implying that the solution of the two phase equation became multiple valued in saturation. Buckley and Leverett crossed this hurdle by suggesting the shock front theory. The saturation of the shock front should be therefore determined. This can be performed by Welge's method or by the material balance technique. This lead to a realistic solution that is considered as exact. Then, the Buckley-Leverett equation was solved numerically using an explicit upwards scheme. The solution obtained was comparable to that of the analytical solution. A smearing was nevertheless present. But, it can be improved by grid refining.

Second, the effect of gravity was investigated. The gravity component can be beneficial by providing stability or disadvantageous. This depends on the dip angle and its direction. The original Buckley-Leverett equation was then modified to account for the capillarity. The latter was solved only numerically in an explicit scheme as it is not possible to solve it analytically. The capillary pressure effects were then observed on the saturation profile, They are highly dependent on ε factor.

5.2 Future Work

Buckley-Leverett theory is a reliable theory and is a key model in the prediction of waterflooding. However, its use is limited since it requires many conditions related to the assumptions to be satisfied. Therefore, treating other real scenarios would be of an important interest. For example, providing a model for fractured reservoirs and accounting for low salinity effects should be considered.

Buckley-Leverett problem should also be tackled from another side. It is interesting to understand the compatibility of the planned injected water with the reservoir's connate water, the possible interactions between the injected water and the reservoir rock and the measures needed to remove oxygen, bacteria, and undesirable chemicals.

Chapter 6

References

- Abidullah ARABZAI, Shigeo HONMA. *Numerical Simulation of the Buckley-Leverett Problem*. 2013.
- Abubaker H. Alagorni, Zulkefli Bin Yaacob, and Abdurahman H. Nour. "An Overview of Oil Production Stages: Enhanced Oil." 2015.
- Adler, P.M. *Multiphase Flow in Porous Media*. Springer Science+Business Media Dordrecht, 1995.
- Ahmed, Tarek. *Reservoir Engineering Handbook Second Edition*. 2001.
- Bentsen, R.G. and Anli, J. "A New Displacement Capillary Pressure Model. J Can Pet Technol 15 (3)." 1976.
- Brooks, R.H. and Corey, A.T. "Hydraulic properties of porous media. Hydrology Paper No. 3." 1964.
- Buckley, S. E., & and M. C. Leverett. "Mechanism of Fluid Displacement in Sands." 1942.
- Clement, William P. *Writing and Thinking Well*. 2 February 2008. <http://cgiss.boisestate.edu/~billc/Writing/writing.html> (accessed July 13, 2016).
- Dake, L.P. *Fundamentals of Reservoir Engineering*. Elsevier, 1978.
- . *The Practice of Reservoir Engineering (Revised Edition)*. Elsevier, 2001.
- Dykstra, H. and parsons, R.L. *The Prediction of Oil recovery by Waterflooding*. 1950.
- Fayers, F. L., and Sheldon, J. W. *The Effect of Capillary Pressure and Gravity on Two-phase Fluid Flow in Porous Medium*. 1959.

- Gottfried, B. S., Gullinger and Snyder. *Numerical Solution of the Equations for One-dimensional Multiphase Flow in Porous Media*. 1966.
- H.M. Goda, P. Behrenbruch. "Using a Modified Brooks-Corey Model to Study Oil-Water Relative Permeability for Diverse Pore Structures ." 2004.
- Helvig, Ole Skretting. "Models for water flooding, imbibition and coupled fracture-matrix flow in a fractured reservoir ." 2013.
- Helvig, Per Kristian Skretting & Ole Skretting. "The two-phase porous media equation in 1D, A bachelor-thesis in petroleum engineering." 2011.
- Hiatt, N.W. *Injected-fluid Coverage of Multi-well Reservoirs with Permeability*. 1958.
- Hirasaki, George J. *Chapter 7: Two Phase, One Dimensional Displacement*. 2009.
- Kazemi, Hossein. *Reservoir Simulation I*. 2009.
- M.Summer. *Handbook of Soil Science*. 1999.
- P.Francis. *ANU*. 1999.
- Rosland, Finn Arthur. "Modelling of water-oil flow in porous reservoirs including effects from gravity, capillary pressure and water-rock chemistry ." 2013.
- Stiles, W.E. *Use of Permeability Distribution in Water-flood Calculations*. 1949.
- Swiss Academic Software. *Citavi - Organize your knowledge. Reference management, knowledge organization, and task planning*. n.d. <https://www.citavi.com/> (accessed May 24, 2016).
- Thomeer, J.H.M. "Introduction of a Pore Geometrical Factor Defined by the Capillary Pressure Curve. J Pet Technol." 1960.
- Warren, J.E. and Cosgrove, J.J. *Prediction of Waterflood Behavior in a Stratified*. 1964.
- Weizhong LUO, B.S. "Saturation Profiles From Petroleum Reservoir Simulation, Studies Compared with Buckley-Leverett Results." 1986.
- Welge, Henry J. "A Simplified Method for Computing Oil Recovery by Gas or Water Drive." 1952.
- Wu, Yu-Shu. *Multiphase Fluid Flow in Porous and Fractured Reservoirs*. Elsevier, 2016.

Appendix A

Reliability of Continuum Fluid Mechanics

A.1 Knudsen Number

Knudsen number Π_{kn} is the ratio of the mean free path of fluid molecules over a representative length scale. The number is used as a reference for preferring continuum fluid mechanics as a modeling tool. Specifically, if Π_{kn} is greater than or equal to unity, then the mean free path of the fluid molecules is of the order of magnitude of the length scale and thus continuum fluid mechanics does not provide a reliable approximation to describe fluid flow. On the contrary, if Π_{kn} is less than unity, then the mean free path is of the order of magnitude of the length scale and hence continuum fluid mechanics does provide a good approximation to describe flow. (Adler 1995)

In the following, whether continuum fluid mechanics can be used effectively or not to describe waterflooding will be justified.

A.2 Mean free path of water molecules

Consider a macroscopic amount of water. Then, the specific number n , the number of molecules per unit mass of water is the ratio between Avogadro's constant N_A and the molar mass of water \hat{m} and hence the number density ρ_N , the number of molecules per unit volume of water is the specific number times water mass density ρ :

$$\rho_N = \frac{\rho N_A}{\hat{m}}$$

Plugging in approximate values for the quantities in the previous equation, we see that

$$\begin{aligned}\rho_N &\sim \frac{1g/cm^3 \times 6 \cdot 10^{23} mol^{-1}}{20g/mol} \\ &\sim 3 \cdot 10^{22} cm^{-3}\end{aligned}$$

Where the symbol \sim is to be read as «is in the order-of-magnitude of».

Suppose now that the spacing between hydrogen and oxygen in a water molecule is in the order of Bohr's radius:

$$r \sim 10^{-8} \text{ cm}$$

Then, estimate the collision cross-section of the molecule as its cross section, a assuming it be a mathematical ball:

$$\begin{aligned} a &\sim r^2 \sim (10^{-8} \text{ cm})^2 \\ &\sim 10^{-16} \text{ cm}^2 \end{aligned}$$

Notice that, since performing a BOTE calculation, (P.Francis 1999) we have dropped the circle constant π from the exact equation for the cross section of a ball; *viz.*, we have mapped $a = \pi r^2$ to $a \sim r^2$. Finally, the mean free path λ (the average distance traveled by a moving particle between successive impacts) of the molecule is

$$\begin{aligned} \lambda &\sim \frac{1}{a \rho_N} \sim \frac{1}{10^{-16} \text{ cm}^2 \times 3 \cdot 10^{22} \text{ cm}^{-3}} \\ &\sim 3 \cdot 10^{-7} \text{ cm} \end{aligned}$$

That is, the distance a water molecule travels between collisions with other molecules is in the order of 10^{-7} cm .

A.3 Porous size of a reservoir

To completely determine Knudsen number, we need to estimate a « representative length scale». In the case of waterflooding, it seems reasonable to choose as representative length scale the porous size of the material that composes the reservoir.

Now, porous sizes are challenging to estimate, because there is no functional relation between a macroscopic property and porous size. For instance, there is no relation between porosity or permeability and porous size, as one would expect. For this reason, the quantity must be directly measured. Table I summarizes measured ranges of pore sizes in soils. There in, we are particularly interested in two types, for they are relevant to the current work:

1. The mesopore type, which is the type with the largest pore size. It is also known as storage pore for its ability to store water. The capillary forces among pores are not too great to immobilize water. (M.Summer 1999)

Table 1: Pore types in soils

Pore type	Pore size range
Macropore	$>75 \mu\text{m}$
Mesopore	$30 \mu\text{m}$ to $75 \mu\text{m}$
Micropore	$5 \mu\text{m}$ to $30 \mu\text{m}$
Ultramicropore	$0.1 \mu\text{m}$ to $30 \mu\text{m}$

2. The micropore type, which is the type whose pores are sufficiently small to yield capillary forces that immobilize water. . (M.Summer 1999)

Hence, we hypothesize that the effective pore size of an oil reservoir should be between the sizes of meso- and micropores. Thus, if we let S stand for pore size, then we have that

$$S \sim \sqrt{5 \mu\text{m} \times 30 \mu\text{m}}$$

$$\sim 10^{-3} \text{ cm}$$

A.4 Knudsen number for waterflooding

We are now in position of estimate the Knudsen number for waterflooding, as the ratio of the mean free path of water molecules and the average pore size of reservoirs:

$$\Pi_{kn} \sim \frac{\lambda}{s} \sim \frac{3 \cdot 10^{-7} \text{ cm}}{10^{-3} \text{ cm}} \sim 10^{-4}$$

$$<< 1$$

That is, since Π_{kn} is much less than unity, the pore size of a reservoir is much larger than the average mean path of water molecules, which means that continuum fluid mechanics – through the Navier-Stokes equations, Darcy's law, and, their off-spring, the fractional flow and frontal advance equations– provide a good approximation to predict waterflooding.

Appendix B

Matlab Code for Analytical Solution

```
%input data
no = input('Set a value for Corey exponent no ? ');
nw = input('Set a value for Corey exponent nw ? ');
M = input('What is the viscosity ratio ? ');
KRW=input('What is the end point relative Permeability of water? ');
KRO=input('What is the end point relative Permeability of oil ? ');
Swi= input('What is the initial water saturation? ');
Sor= input('What is the residual oil saturation? ');
T = input('Please enter the elapsed time ');
%Corey relative permeabilities
function [rel_w,rel_o] = rel_perm(s1,no,nw,KRW,KRO,Swi,Sor)
Swn = (s1 - Swi) ./ (1 - Swi - Sor);
rel_w = zeros(size(Swn));
rel_o = zeros(size(Swn));
rel_w = KRW .* (Swn.^nw) ;
rel_o = KRO.*((1-Swn).^no);
figure(1)
s = Swi:0.01:(1-Sor);
[kw,ko] = rel_perm(s,no,nw,KRW,KRO,Swi,Sor) ;
plot(s,kw,'LineWidth',2);
hold on
plot(s,ko,'LineWidth',2);
hold on
axis([0 1 0 1]);
drawnow;
title('Corey Relative Permeabilities');
xlabel('Water Saturation Sw')
ylabel('Relative Permeability')
legend('Relative Permeability of Water','Relative permeability of oil')
grid on
%Fractional flow curve
function f=Fractional_Flow(sat,M,no,nw,KRW,KRO,Swi,Sor)
f = zeros(size(sat));
[rel_w,rel_o] = rel_perm(sat,no,nw,KRW,KRO,Swi,Sor);
f = rel_w./(rel_w + M * rel_o);
figure(2)
s = Swi:0.01:(1-Sor) ;
fw = Fractional_Flow(s,M,no,nw,KRW,KRO,Swi,Sor);
plot(s,fw,'-','LineWidth',2);
```

```

hold on
axis([0 1 0 1]);
drawnow;
grid on
xlabel('Water Saturation')
ylabel('fw')
hold off
%Fractional flow derivative
function f=derivative_fractional_flow(s1,M,no,nw,KRO,KRW,Swi,Sor)
f = zeros(size(s1));
Swn = (s1 - Swi) ./ (1 - Swi - Sor);
f = ((M .* KRO .* KRW .* ((1-Swn).^(no-1)) .* (Swn.^(nw-1))) .* ((1-Swn).^nw + no.*Swn)) ./ ((KRW .* Swn .^nw + KRO .* M .* (1 - Swn).^no).^2) ;
figure(3)
s = 0:0.01:1;
plot(s, derivative_fractional_flow(s,M,no,nw,KRO,KRW,Swi,Sor), '-');
axis([0 2 0 3]);
hold on
drawnow;
title('Derivative of fractional Flow');
xlabel('Water Saturation')
ylabel('Df/DS')
hold off
% Saturation movement, unphysical solution
function f = saturation_profile(s1,M,no,nw,KRO,KRW,Swi,Sor,T)
f = zeros(size(s1));
Swn = (s1 - Swi) ./ (1 - Swi - Sor);
f = T * ((M .* KRO .* KRW .* ((1-Swn).^(no-1)) .* (Swn.^(nw-1))) .* ((1-Swn).^nw + no.*Swn)) ./ ((KRW .* Swn .^nw + KRO .* M .* (1 - Swn).^no).^2) ;

figure(4)
plot(saturation_profile(s,M,no,nw,KRO,KRW,Swi,Sor,T),s), '-';
axis([0 1.2 0 1]);
hold on
drawnow;
title('Saturation Profile, unphysical solution');
xlabel('Position x')
ylabel('Water Saturation')
grid on

```

Appendix C

Matlab Code for Numerical Solution

```
%input data
no = input('Set a value for Corey exponent no ? ');
nw = input('Set a value for Corey exponent nw ? ');
M = input('What is the viscosity ratio ? ');
KRW=input('What is the end point relative Permeability of water? ');
KRO=input('What is the end point relative Permeability of oil ? ');
Swi= input(' What is the initial water Saturation? ');
Sor= input(' What is the residual oil Saturation? ');
% Initial condition
S_init = @(x) ( x <= 0)*(1-Sor) + (0<x<=1)* Swi;
% Boundary condition reSultat
S_edge = S_init(-1);
%Fractional flow curve
Fractional_flow =@(S) KRW.*(((S-Swi)./(1-Swi-Sor)).^nw)./(KRW.*(((S-Swi)./(1-Swi-Sor)).^nw)+KRO.*((1-((S-Swi)./(1 - Swi - Sor))).^no)) );
% Spatial and temporal grid
x = linspace(0, 1, 101);
dx = x(2) - x(1);
t_max = 1;
dt = t_max / 50;
% ReSet initial condition
S = S_init(x);
fw = zeros(size(S));
% Satisfy the CFL condition
SS = 0:0.01:1;
v = diff( Fractional_flow(SS)) ./ diff(SS);
CFL = 0.5; dt = CFL*dx/max(abs(v));
% Time stepping
t = 0;
while t < t_max
    t = t + dt;
    % Upwind advective flux, harmonic gravity flux
    F_w = Fractional_flow(S);
    for i = 1:length(F_w)
        fw(i) = F_w(i) ;
    end
    % Explicit time stepping
    S_old = S;
    for i = 2:length(S)
        S(i) = S_old(i) - (dt /dx)*(fw(i) - fw(i-1));
    end
end
```

```
    plot(x,S)
    axis([0 1 0 1]);
    pause(0.01);
end
```


Appendix D

Generalized Buckley-Leverett Problem (Gravity Effect)

D.1 Input Data

Absolute Permeability	$K = 5 \times 10^{-13}$
Oil viscosity	$\mu_o = 0.7 \text{ Pa} \cdot \text{S}^{-1}$
Water Viscosity	$\mu_w = 0.35 \text{ Pa} \cdot \text{S}^{-1}$
Mobility of oil	$\lambda_o = 1428.57 \text{ m}^2 / \text{Pa} \cdot \text{s}$
Water Density	$\rho_w = 1000 \text{ kg/m}^3$
Oil density	$\rho_o = 850 \text{ kg/m}^3$
Gravitational constant	$g = 9.81 \text{ m/S}^2$
Dip angle	$\theta = 25^\circ$
Total velocity	$U_t = 1.15 \times 10^{-7} \text{ m/S}$
Gravity Number	$N_G = 3.83$

D.2 Matlab Code

```
%input data  
  
no = input(' Set a value for Corey exponent no ? ');  
nw = input(' Set a value for Corey exponent nw ? ');  
M = input(' What is the viscosity ratio ? ');  
KRW= input(' What is the end point relative Permeability of water? ');
```

```

KRO= input(' What is the end point relative Permeability of oil  ?
');
Swi= input(' What is the initial water saturation? ');
Sor= input(' What is residual oil saturation?      ');

% Water Fractional flow equation
function f=Fractional_Flow(sat,M,no,nw,KRW,KRO,Swi,Sor,NG)
f = zeros(size(sat));
[rel_w,rel_o] = rel_perm(sat,no,nw,KRW,KRO,Swi,Sor);
f =( rel_w./(rel_w + M * rel_o) ).*(1- NG .* rel_o) ;

%Fractional flow curve
%Plot f(s)

NG=-3.8;
while NG<4 ;
figure(20)
s = Swi:0.01:(1-Sor) ;
fw = Fractional_Flow(s,M,no,nw,KRW,KRO,Swi,Sor,NG);
%subplot(2,2,2)
plot(s,fw,'-','LineWidth',2);
axis([0 1 -0.2 1.2]);

hold on
drawnow;

grid on
xlabel('Water Saturation')
ylabel('fw')
%hold off
NG=NG+3.8;
end

```